NASA-TM-84636 19830017254

NASA Technical Memorandum 84636

Nucleon and Deuteron Scattering Cross Sections From 25 MeV/Nucleon to 22.5 GeV/Nucleon

Lawrence W. Townsend, John W. Wilson, and Hari B. Bidasaria

MAY 1983

25

25th Anniversary
1958-1983

NASA

Nucleon and Deuteron Scattering Cross Sections From 25 MeV/Nucleon to 22.5 GeV/Nucleon

Lawrence W. Townsend and John W. Wilson
Langley Research Center
Hampton, Virginia

Hari B. Bidasaria
Old Dominion University
Norfolk, Virginia

INTRODUCTION

Particles lighter than helium comprise over 90 percent of the particle abundance of cosmic radiation (ref. 1). As a result, knowledge of nucleon and deuteron interactions and transport in bulk matter is required for accurate analyses of space radiation shielding requirements. In previous work (refs. 2 to 11), a comprehensive nuclear interaction theory capable of describing incident particle absorption, total, and abrasion cross sections has been developed for use as input into a transport theory under concurrent development (refs. 12 and 13). In the present report, this interaction theory is used to generate tables of nucleon and deuteron cross sections for incident energies of interest in cosmic-ray shielding studies. As such, this work presents an improved and updated version of the original tables presented in reference 4. Comparisons with available experimental data for nucleon-nucleus and deuteron-nucleus collisions are also made.

SYMBOLS

A   nuclear mass number

a   parameter in harmonic well function, fm

$B(e)$ average slope parameter of nucleon-nucleon scattering amplitude, fm^2

$\vec{b}$ projectile impact parameter vector, fm

c   Woods-Saxon surface diffuseness, fm

E_{lab} projectile laboratory energy per unit mass, GeV/nucleon

e   two-nucleon kinetic energy in their center of mass frame, GeV

$Im\ \chi(\vec{b})$ imaginary part of eikonal phase shift function

$\vec{k}$ projectile momentum vector relative to target, fm^{-1}

m   nucleon mass, kg

R   radius at half density, fm

$Re\ \chi(\vec{b})$ real part of eikonal phase shift function

$\vec{r}$ position vector, fm

r_N nucleon root-mean-square charge radius, fm

s   defined in equation (13)

t   skin thickness, fm

$\tilde{t}$ average two-nucleon transition amplitude, MeV

$U(\vec{x})$ reduced potential, MeV^2

$W(\vec{x})$ optical potential (defined in eq. (5)), MeV

$\vec{x}$ relative position vector of projectile ($\vec{x} = \vec{b} + \vec{z}$), fm

$\vec{y}$ two-nucleon relative position vector, fm

$\vec{z}$ position vector of projectile in beam direction, fm

$\alpha(e)$ average ratio of real part to imaginary part of nucleon-nucleon scattering amplitude

β defined in equation (17)

γ harmonic well distribution parameter (see eq. (11))

$\vec{\xi}_T$ collection of constituent relative coordinates for target, fm

ρ nuclear density, fm^{-3}

ρ_0 normalization constant in equations (11) and (14), fm^{-3}

$\sigma(e)$ average nucleon-nucleon total cross section, fm^2 or mb

σ_{abs} absorption cross section, fm^2 or mb

σ_{tot} total cross section, fm^2 or mb

$\chi(\vec{b})$ eikonal phase shift function

Subscripts:

A   matter

c   charge

N   nucleon

n   neutron

P   projectile

p   proton

T   target

Abbreviations:

HW   harmonic well

WS   Woods-Saxon

Arrows over symbols indicate vectors.

2

THEORETICAL DEVELOPMENT

From eikonal scattering theory, the collision total and absorption cross sections are given by

$$\sigma_{tot} = 4\pi \int_0^\infty \left\{1 - \exp[-Im\ \chi(\vec{b})]\ \cos[Re\ \chi(\vec{b})]\right\} b\ db \tag{1}$$

and

$$\sigma_{abs} = 2\pi \int_0^\infty \left\{1 - \exp[-2Im\ \chi(\vec{b})]\right\} b\ db \tag{2}$$

where the complex phase function, in terms of the reduced potential U is

$$\chi(\vec{b}) = -\frac{1}{2k} \int_{-\infty}^\infty U(\vec{b},z)\ dz \tag{3}$$

For composite particle scattering, the reduced potential is written as

$$U(\vec{x}) = 2mA_P A_T (A_P + A_T)^{-1}\ W(\vec{x}) \tag{4}$$

where m is the nucleon mass, A_P is the nuclear mass number of the projectile, and A_T is the nuclear mass number of the target. From references 4 and 5, the nucleus-nucleus optical potential is

$$W(\vec{x}) = A_P A_T \int d^3\vec{\xi}_T\ \rho_T(\vec{\xi}_T) \int d^3\vec{y}\ \rho_P(\vec{x}+\vec{y}+\vec{\xi}_T)\ \tilde{t}(e,\vec{y}) \tag{5}$$

In equation (5), $\tilde{t}$ is the constituent-averaged energy-dependent two-body transition amplitude

$$\tilde{t}(e,\vec{y}) = -\left(\frac{e}{m}\right)^{1/2} \sigma(e)[\alpha(e) + i][2\pi\ B(e)]^{-3/2} \exp\left[\frac{-y^2}{2B(e)}\right] \tag{6}$$

The correct nuclear density distributions ρ_P and ρ_T to use in equation (5) are the nuclear ground state, single-particle number densities for the collision pair. Since these are not experimentally known, the number densities are obtained from their experimental charge density distributions by assuming

$$\rho_C(\vec{r}) = \int \rho_N(\vec{r}') \, \rho_A(\vec{r}+\vec{r}') \, d^3\vec{r}' \tag{7}$$

where ρ_C is the nuclear charge distribution, ρ_N is the nucleon charge distribution, and ρ_A is the desired nuclear single-particle density. All density distributions in equation (7) are normalized to unity. The nucleon charge distribution is taken to be the usual Gaussian form

$$\rho_N(\vec{r}) = \left(\frac{3}{2\pi r_N^2}\right)^{3/2} \exp\left(\frac{-3r^2}{2r_N^2}\right) \tag{8}$$

where the nucleon root-mean-square charge radius r_N (ref. 14) is

$$r_N^2 = 0.76 - 0.11 \frac{N}{Z} \tag{9}$$

where N is the neutron number, and Z is the proton number for the nucleus under consideration.

When the projectile is a nucleon, equation (7) yields a delta function for ρ_A,

$$\rho_A(\vec{r}+\vec{r}') = \delta(\vec{r}+\vec{r}') \tag{10}$$

since ρ_C and ρ_N are identical. For nuclei lighter than neon (A < 20), the nuclear charge distribution is the harmonic well (HW) form given by reference 15

$$\rho_C(r) = \rho_O\left[1 + \gamma\left(\frac{r}{a}\right)^2\right] \exp\left(\frac{-r^2}{a^2}\right) \tag{11}$$

where ρ_O is the normalization constant, r is the radial coordinate, and a and γ are charge parameters. Values for a and γ, used herein, are listed in

table 1. Substituting equations (8) and (11) into equation (7) yields (ref. 8)

$$\rho_A(r) = \frac{\rho_o a^3}{8s^3}\left(1 + \frac{3\gamma}{2} - \frac{3\gamma a^2}{8s^2} + \frac{\gamma a^2 r^2}{16s^4}\right)\exp\left(\frac{-r^2}{4s^2}\right)$$ (12)

where

$$s^2 = \frac{a^2}{4} - \frac{r_N^2}{6}$$ (13)

For neon and heavier nuclei (A > 20), the nuclear charge distribution is taken to be the Woods-Saxon (WS) form given by reference 5

$$\rho_c(r) = \frac{\rho_o}{1 + \exp[(r - R)/c]}$$ (14)

where R is the radius at half density, and the diffuseness c is related to the nuclear skin thickness t through

$$c = \frac{t}{4.4}$$ (15)

Values for R and t, used herein, are listed in table 1. Most values are taken from reference 15. Inserting equations (8) and (14) into equation (7) yields, after some simplification (ref. 5), a number density ρ_A which is of the WS form (see eq. (14)) with the same R, but different overall normalization factor ρ_o and surface thickness. The latter is given by

$$t_A = \frac{8.8r_N}{3^{1/2}}\left[\ln\left(\frac{3\beta - 1}{3 - \beta}\right)\right]^{-1}$$ (16)

where

$$\beta = \exp\left(\frac{4.4r_N}{t_c 3^{1/2}}\right)$$ (17)

with t_c denoting the charge skin thickness obtained by solving equation (15) after substitution of the charge distribution surface diffuseness values c listed in reference 15.

Nucleon-Nucleon Scattering Parameters

The nucleon-nucleon scattering parameters $\alpha(e)$, $\sigma(e)$, and $B(e)$ used in the energy-dependent two-body transition amplitude (eq. (6)) are obtained by performing a spline interpolation of values taken from various compilations (refs. 16 to 20). The results are displayed in figures 1 to 6 as a function of incident energy. No curves for neutron-neutron scattering parameters are displayed, since little or no experimental data exist for these collisions. For computational purposes, it is assumed that the neutron-neutron parameters are adequately represented by the proton-proton scattering parameters for each energy considered. Details of the constituent-averaging of equation (6) are given in reference 4.

RESULTS

Using the formalism described in the previous sections, total and absorption cross sections for nucleons and deuterons colliding with various target nuclei have been calculated. The results are given in tables 2 to 5. The target nuclei were selected for their applicability to cosmic-ray shielding studies. No significant errors are expected for values obtained by interpolating between the target mass numbers of nuclei displayed in the tables.

Nucleon-Nucleus Cross Sections

Comparisons between the theoretical predictions for nucleon-nucleus scattering, from tables 2 and 3 and representative experimental results (refs. 18 and 21) are displayed in figures 7 to 14. For the absorption cross sections, the agreement is excellent at all energies. For incident energies above 100 MeV/nucleon, the predicted values for total cross sections are typically within 5 percent of the experimental values. For energies less than 100 MeV/nucleon, however, the theory considerably underestimates the total cross sections for each of the displayed target nuclei (see figs. 11 to 14). These discrepancies are likely due to the questionable validity of the eikonal approximation at low energies, as well as to uncertainties in the nucleon-nucleon scattering parameters, particularly $\alpha(e)$ (see ref. 22). Additional sources of possible errors at these lower energies include the neglect of off-shell and spin-dependent effects.

Deuteron-Nucleus Cross Sections

Table 6 contains theoretical cross-section predictions for deuteron-helium and deuteron-carbon scattering along with experimental results from reference 23. Comparison of the predicted and experimental values shows excellent agreement (within 3 to 11 percent). However, the theoretical predictions are all higher than the listed experimental results. These discrepancies, aside from possible contributions resulting from the neglect of off-shell effects, spin-dependent effects, and/or Pauli correlations (ref. 8), may result from the choice of a single Gaussian form for the deuteron density distribution, rather than a more exact sum-of-Gaussians form (ref. 24). The latter, however, requires replacing the single Gaussian term, used herein, by a sum of up to 36 Gaussian terms.

CONCLUDING REMARKS

Tables of nucleon-nucleus and deuteron-nucleus total and absorption cross sections for use in cosmic-ray transport and shielding studies have been generated over the energy range from 25 MeV/nucleon to 22.5 GeV/nucleon. Comparisons between the calculated cross sections and experimental data show excellent agreement except for low energy (<100 MeV) nucleon-nucleus total cross sections, where the lack of substantial agreement is likely due to the questionable validity of the eikonal formalism and to the poorly determined values for the experimental nucleon-nucleon scattering parameters.

Langley Research Center
National Aeronautics and Space Administration
Hampton, VA 23665
March 31, 1983

REFERENCES

1. Haffner, James W.: Radiation and Shielding in Space. Academic Press, 1967, pp. 1-70.

2. Wilson, John W.: Composite Particle Reaction Theory. Ph.D. Diss., The College of William and Mary in Virginia, June 1975.

3. Wilson, J. W.: Multiple Scattering of Heavy Ions, Glauber Theory, and Optical Model. Phys. Lett., vol. B52, no. 2, Sept. 1974, pp. 149-152.

4. Wilson, John W.; and Costner, Christopher M.: Nucleon and Heavy-Ion Total and Absorption Cross Section for Selected Nuclei. NASA TN D-8107, 1975.

5. Wilson, J. W.; and Townsend, L. W.: An Optical Model for Composite Nuclear Scattering. Canadian J. Phys., vol. 59, no. 11, Nov. 1981, pp. 1569-1576.

6. Townsend, Lawrence W.: Optical-Model Abrasion Cross Sections for High-Energy Heavy Ions. NASA TP-1893, 1981.

7. Townsend, L. W.; and Wilson, J. W.: Comment on "Nucleus-Nucleus Total Reaction Cross Sections." Phys. Rev., ser. C, vol. 25, no. 3, Mar. 1982. pp. 1679-1681.

8. Townsend, Lawrence W.: Harmonic Well Matter Densities and Pauli Correlation Effects in Heavy-Ion Collisions. NASA TP-2003, 1982.

9. Townsend, L. W.; Wilson, J. W.; and Bidasaria, H. B.: On the Geometric Nature of High-Energy Nucleus-Nucleus Reaction Cross Sections. Canadian J. Phys., vol. 60, no. 10, Oct. 1982, pp. 1514-1518.

10. Bidasaria, Hari B.; and Townsend, Lawrence W.: Analytic Optical Potentials for Nucleon-Nucleus and Nucleus-Nucleus Collisions Involving Light and Medium Nuclei. NASA TM-83224, 1982.

11. Townsend, Lawrence W.; and Bidasaria, Hari B.: Improvements to the Langley HZE Abrasion Model. NASA TM-84542, 1982.

12. Wilson, John W.; and Lamkin, Stanley L.: Perturbation Theory for Charged-Particle Transport in One Dimension. Nucl. Sci. & Eng., vol. 57, no. 4, Aug. 1975, pp. 292-299.

13. Wilson, John W.: Analysis of the Theory of High-Energy Ion Transport. NASA TN D-8381, 1977.

14. Satchler, G. R.; and Love, W. G.: Folding Model Potentials From Realistic Interactions for Heavy-Ion Scattering. Phys. Rep., vol. 55, no. 3, Oct. 1979, pp. 183-254.

15. De Jager, C. W.; De Vries, H.; and De Vries, C.: Nuclear Charge- and Magnetization-Density-Distribution Parameters From Elastic Electron Scattering. At. Data & Nucl. Data Tables, vol. 14, no. 5/6, Nov./Dec. 1974, pp. 479-508.

16. Amirkhanov, I. V.; Zul'karneev, R. Ya.; Murtazaev, H.; Nadejdin, V. S.; and Satarov, V. I.: $d\sigma(0°)/d\Omega$, $\sigma_{tot\ el}$ and ReA(0°) for Elastic pp-Scattering in the 1-1000 MeV Energy Range. High-Energy Physics and Nuclear Structure, Gunnar Tibell, ed., American Elsevier Pub. Co., Inc., 1974, pp. 47-50.

17. Benary, Odette; Price, Leroy R.; and Alexander, Gideon: NN and ND Interactions (Above 0.5 GeV/c) - A Compilation. UCRL-20000 NN, Lawrence Radiation Lab., Univ. California, Aug. 1970.

18. Schopper, H., ed.: Elastic and Charge Exchange Scattering of Elementary Particles. Landolt-Börnstein Numerical Data and Functional Relationships in Science and Technology, Group I, Volume 7, Springer-Verlag, 1973.

19. Schopper, H., ed.: Elastic and Charge Exchange Scattering of Elementary Particles. Landolt-Börstein Numerical Data and Functional Relationships in Science and Technology, Group I, Volume 9, Springer-Verlag, 1980.

20. Binstock, Judith: Parametrization of σ_{tot}, $\sigma(\Theta)$, $P(\Theta)$ for 25-100 MeV np Elastic Scattering. Phys. Rev., ser. C, vol. 10, no. 1, July 1974, pp. 19-23.

21. Barashenkov, V. S.; Gudima, K. K.; and Toneev, V. D.: Cross Sections for Fast Particles and Atomic Nuclei. Progr. Phys., vol. 17, no. 10, 1969, pp. 683-725.

22. Bidasaria, H. B.; Townsend, L. W.; and Wilson, J. W.: Theory of Carbon-Carbon Scattering From 200 to 290 MeV. J. Phys. G.: Nucl. Phys., vol. 9, no. 1, Jan. 1983, pp. L17-L20.

23. Jaros, J.; Wagner, A.; Anderson, L.; Chamberlain, O.; Fuzesy, R. Z.; Gallup, J.; Gorn, W.; Schroeder, L; Shannon, S.; Shapiro, G.; and Steiner, H.: Nucleus-Nucleus Total Cross Sections for Light Nuclei at 1.55 and 2.89 GeV/c per Nucleon. Phys. Rev., ser. C, vol. 18, no. 5, Nov. 1978, pp. 2273-2292.

24. Wilson, John W.: Intermediate Energy, Nucleon-Deuteron Elastic Scattering. Nucl. Phys., vol. B66, Dec. 17, 1973, pp. 221-244.

TABLE 1. – NUCLEAR CHARGE DISTRIBUTION PARAMETERS
FROM ELECTRON SCATTERING DATA

Nucleus	Distribution (*)	γ (HW) or t, fm (WS)	a, fm (HW) or R, fm (WS)
^{2}H	HW	0	1.71
^{4}He	HW	0	1.33
^{7}Li	HW	.327	1.77
^{9}Be	HW	.611	1.791
^{11}B	HW	.811	1.69
^{12}C	HW	1.247	1.649
^{14}N	HW	1.291	1.729
^{16}O	HW	1.544	1.833
^{20}Ne	WS	2.517	2.74
^{27}Al	WS	2.284	3.07
^{40}Ar	WS	2.693	3.47
^{56}Fe	WS	2.611	3.971
^{64}Cu	WS	2.504	4.20
^{80}Br	WS	2.306	4.604
^{108}Ag	WS	2.354	5.139
^{138}Ba	WS	2.621	5.618
^{208}Pb	WS	2.416	6.624

*HW – harmonic well (eq. (11)); WS – Woods-Saxon
(eq. (14)).

TABLE 2. - NUCLEON-NUCLEUS TOTAL CROSS SECTION

Nucleon-nucleus total cross section, mb, for -

Energy, MeV/amu	He	C	O	Al	Ar	Fe	Cu	Br	Ag	Ba	Pb
25.	325.	765.	972.	1170.	1679.	1965.	2059.	2078.	2678.	3311.	4109.
50.	258.	635.	810.	1012.	1429.	1710.	1813.	1893.	2425.	2980.	3784.
75.	226.	573.	735.	944.	1327.	1601.	1709.	1813.	2318.	2847.	3645.
100.	197.	511.	659.	885.	1242.	1514.	1623.	1744.	2225.	2728.	3520.
125.	175.	460.	596.	833.	1174.	1449.	1562.	1698.	2162.	2647.	3434.
150.	157.	416.	539.	777.	1104.	1379.	1497.	1649.	2103.	2576.	3362.
175.	140.	371.	482.	710.	1016.	1286.	1405.	1572.	2014.	2475.	3263.
200.	125.	330.	429.	638.	917.	1172.	1287.	1458.	1879.	2321.	3099.
225.	117.	309.	402.	601.	865.	1111.	1222.	1393.	1800.	2228.	2994.
250.	112.	296.	385.	576.	829.	1068.	1176.	1345.	1741.	2157.	2913.
275.	109.	287.	373.	557.	802.	1034.	1140.	1305.	1691.	2096.	2842.
300.	107.	281.	366.	546.	785.	1014.	1118.	1280.	1660.	2057.	2796.
350.	104.	273.	355.	530.	762.	985.	1085.	1245.	1616.	2003.	2729.
400.	107.	279.	362.	537.	770.	993.	1093.	1249.	1620.	2006.	2732.
500.	116.	302.	391.	570.	812.	1042.	1141.	1294.	1675.	2067.	2804.
600.	126.	324.	419.	603.	855.	1092.	1193.	1342.	1734.	2135.	2885.
700.	133.	340.	440.	626.	886.	1128.	1229.	1378.	1777.	2186.	2943.
800.	136.	348.	449.	638.	903.	1146.	1249.	1397.	1801.	2214.	2975.
900.	138.	354.	456.	647.	915.	1160.	1263.	1412.	1819.	2237.	2999.
1000.	140.	358.	462.	654.	925.	1172.	1275.	1424.	1835.	2256.	3020.
1250.	145.	367.	473.	670.	948.	1198.	1304.	1454.	1871.	2300.	3070.
1500.	147.	372.	479.	678.	958.	1211.	1317.	1470.	1889.	2321.	3094.
1750.	148.	373.	480.	681.	962.	1216.	1323.	1477.	1897.	2331.	3105.
2000.	149.	374.	482.	684.	966.	1220.	1328.	1483.	1904.	2339.	3115.
2500.	150.	374.	481.	685.	967.	1222.	1331.	1488.	1910.	2345.	3123.
3000.	149.	373.	480.	684.	966.	1221.	1330.	1487.	1909.	2344.	3122.
3500.	149.	371.	477.	681.	962.	1216.	1326.	1484.	1904.	2339.	3117.
4000.	148.	368.	473.	676.	956.	1210.	1318.	1477.	1896.	2329.	3106.
5000.	146.	364.	468.	670.	946.	1199.	1307.	1466.	1883.	2313.	3088.
6000.	145.	361.	465.	666.	941.	1193.	1301.	1459.	1875.	2303.	3078.
7000.	144.	360.	462.	663.	936.	1188.	1295.	1454.	1868.	2295.	3069.
8000.	144.	358.	460.	660.	932.	1183.	1290.	1449.	1862.	2288.	3060.
9000.	143.	356.	458.	657.	928.	1178.	1286.	1444.	1856.	2280.	3051.
10000.	143.	355.	457.	655.	925.	1174.	1281.	1439.	1849.	2272.	3043.
12500.	142.	352.	452.	650.	917.	1165.	1271.	1430.	1837.	2256.	3026.
15000.	142.	350.	449.	646.	910.	1158.	1264.	1423.	1828.	2245.	3013.
17500.	142.	348.	446.	642.	905.	1152.	1257.	1417.	1820.	2235.	3002.
20000.	141.	346.	444.	640.	901.	1147.	1252.	1412.	1814.	2228.	2993.
22500.	141.	345.	443.	638.	898.	1143.	1249.	1409.	1810.	2222.	2987.

TABLE 3. - NUCLEON-NUCLEUS ABSORPTION CROSS SECTION

Nucleon-nucleus absorption cross section, mb, for -

Energy, MeV/amu	He	C	O	Al	Ar	Fe	Cu	Br	Ag	Ba	Pb
25.	190.	435.	552.	652.	948.	1092.	1135.	1117.	1446.	1796.	2192.
50.	144.	344.	438.	540.	773.	913.	963.	987.	1270.	1569.	1965.
75.	124.	302.	386.	490.	699.	836.	888.	929.	1193.	1473.	1866.
100.	108.	269.	345.	449.	641.	775.	829.	880.	1130.	1394.	1785.
125.	100.	250.	321.	425.	606.	739.	793.	850.	1092.	1347.	1735.
150.	95.	238.	306.	410.	585.	716.	770.	831.	1067.	1316.	1704.
175.	91.	229.	295.	398.	567.	698.	752.	815.	1047.	1291.	1678.
200.	88.	222.	286.	389.	554.	683.	737.	803.	1031.	1271.	1657.
225.	85.	217.	279.	381.	543.	672.	726.	793.	1019.	1256.	1641.
250.	84.	213.	274.	376.	535.	664.	717.	785.	1009.	1244.	1629.
275.	83.	210.	271.	373.	530.	658.	712.	780.	1003.	1236.	1621.
300.	82.	209.	270.	371.	527.	655.	709.	777.	999.	1231.	1616.
350.	81.	207.	267.	368.	523.	651.	704.	773.	994.	1225.	1610.
400.	84.	213.	274.	375.	532.	661.	714.	782.	1005.	1236.	1623.
500.	90.	228.	293.	394.	557.	689.	742.	806.	1034.	1270.	1662.
600.	97.	241.	309.	412.	580.	714.	766.	827.	1060.	1300.	1696.
700.	101.	250.	321.	423.	596.	731.	783.	841.	1078.	1321.	1719.
800.	103.	255.	326.	429.	603.	739.	791.	848.	1087.	1331.	1730.
900.	104.	257.	329.	432.	608.	744.	796.	853.	1092.	1337.	1738.
1000.	105.	259.	332.	435.	611.	747.	800.	857.	1097.	1343.	1743.
1250.	107.	263.	336.	440.	617.	754.	807.	864.	1105.	1353.	1753.
1500.	109.	264.	337.	442.	620.	757.	810.	867.	1109.	1357.	1758.
1750.	109.	265.	338.	442.	620.	757.	810.	869.	1110.	1358.	1760.
2000.	109.	264.	337.	442.	620.	757.	811.	869.	1111.	1359.	1760.
2500.	109.	264.	336.	442.	620.	757.	810.	870.	1111.	1359.	1760.
3000.	109.	263.	335.	441.	618.	755.	809.	869.	1109.	1357.	1758.
3500.	109.	262.	334.	440.	616.	753.	807.	867.	1107.	1354.	1756.
4000.	108.	261.	332.	438.	614.	751.	804.	865.	1105.	1351.	1752.
5000.	107.	259.	330.	436.	610.	747.	801.	862.	1101.	1346.	1747.
6000.	107.	258.	329.	435.	609.	745.	799.	860.	1098.	1343.	1744.
7000.	107.	257.	328.	434.	608.	744.	798.	859.	1097.	1342.	1743.
8000.	107.	257.	328.	433.	607.	743.	797.	859.	1097.	1341.	1742.
9000.	107.	257.	327.	433.	606.	743.	796.	859.	1096.	1340.	1742.
10000.	107.	257.	327.	433.	606.	743.	796.	859.	1096.	1340.	1741.
12500.	107.	256.	326.	433.	605.	742.	795.	859.	1095.	1339.	1740.
15000.	107.	256.	326.	433.	604.	741.	795.	859.	1095.	1338.	1740.
17500.	108.	256.	325.	432.	603.	740.	794.	859.	1095.	1337.	1739.
20000.	108.	255.	325.	432.	602.	739.	794.	859.	1094.	1336.	1739.
22500.	108.	255.	325.	432.	602.	739.	794.	859.	1095.	1336.	1739.

TABLE 4. - DEUTERON-NUCLEUS TOTAL CROSS SECTION

Deuteron-nucleus total cross section, mb, for -

Energy, MeV/amu	He	C	O	Al	Ar	Fe	Cu	Br	Ag	Ba	Pb
25.	732.	1357.	1623.	1934.	2529.	2908.	3040.	3153.	3834.	4532.	5530.
50.	558.	1111.	1343.	1651.	2166.	2532.	2669.	2818.	3442.	4077.	5054.
75.	471.	996.	1214.	1518.	1999.	2358.	2496.	2659.	3256.	3863.	4828.
100.	395.	898.	1104.	1405.	1857.	2210.	2348.	2522.	3097.	3680.	4634.
125.	343.	821.	1019.	1324.	1755.	2101.	2239.	2420.	2979.	3545.	4489.
150.	305.	753.	941.	1252.	1667.	2008.	2145.	2330.	2874.	3426.	4361.
175.	271.	681.	857.	1168.	1567.	1904.	2040.	2229.	2758.	3293.	4215.
200.	242.	610.	770.	1072.	1451.	1781.	1917.	2112.	2623.	3139.	4047.
225.	227.	573.	726.	1020.	1386.	1711.	1846.	2044.	2545.	3052.	3951.
250.	217.	550.	696.	984.	1341.	1662.	1796.	1995.	2489.	2988.	3881.
275.	211.	532.	675.	956.	1306.	1622.	1756.	1955.	2442.	2936.	3824.
300.	207.	523.	662.	940.	1284.	1598.	1731.	1930.	2414.	2903.	3787.
350.	201.	507.	643.	914.	1251.	1560.	1691.	1890.	2367.	2850.	3727.
400.	207.	517.	654.	925.	1263.	1572.	1702.	1899.	2377.	2862.	3739.
500.	227.	555.	699.	974.	1324.	1637.	1768.	1962.	2450.	2944.	3828.
600.	247.	593.	744.	1024.	1386.	1704.	1836.	2028.	2526.	3030.	3923.
700.	261.	620.	775.	1059.	1429.	1751.	1883.	2074.	2579.	3091.	3989.
800.	268.	633.	791.	1076.	1451.	1774.	1907.	2097.	2605.	3120.	4022.
900.	272.	642.	801.	1088.	1466.	1790.	1924.	2114.	2625.	3142.	4046.
1000.	276.	649.	810.	1098.	1478.	1804.	1937.	2127.	2640.	3160.	4065.
1250.	283.	664.	829.	1120.	1506.	1835.	1969.	2159.	2677.	3201.	4111.
1500.	286.	671.	837.	1131.	1519.	1849.	1984.	2175.	2694.	3220.	4133.
1750.	287.	673.	839.	1135.	1523.	1854.	1990.	2181.	2701.	3228.	4142.
2000.	287.	675.	842.	1138.	1527.	1859.	1995.	2186.	2707.	3234.	4149.
2500.	286.	675.	841.	1139.	1529.	1861.	1997.	2189.	2710.	3238.	4154.
3000.	285.	672.	839.	1137.	1526.	1858.	1994.	2187.	2708.	3234.	4151.
3500.	283.	669.	835.	1133.	1521.	1853.	1989.	2183.	2702.	3228.	4144.
4000.	280.	664.	829.	1127.	1513.	1845.	1981.	2175.	2693.	3218.	4133.
5000.	277.	657.	821.	1117.	1501.	1832.	1968.	2162.	2679.	3202.	4115.
6000.	275.	653.	816.	1112.	1495.	1825.	1961.	2155.	2671.	3192.	4105.
7000.	273.	650.	812.	1107.	1489.	1819.	1954.	2149.	2664.	3184.	4096.
8000.	272.	647.	808.	1103.	1484.	1813.	1949.	2143.	2657.	3177.	4088.
9000.	271.	644.	805.	1099.	1479.	1808.	1943.	2138.	2651.	3170.	4081.
10000.	270.	641.	802.	1096.	1474.	1802.	1938.	2133.	2646.	3164.	4073.
12500.	267.	636.	795.	1088.	1464.	1792.	1927.	2123.	2634.	3150.	4059.
15000.	265.	631.	789.	1082.	1456.	1783.	1919.	2116.	2625.	3139.	4047.
17500.	264.	627.	784.	1076.	1449.	1776.	1911.	2109.	2616.	3130.	4037.
20000.	262.	624.	780.	1072.	1444.	1770.	1905.	2103.	2610.	3122.	4029.
22500.	262.	623.	778.	1070.	1440.	1766.	1901.	2100.	2605.	3117.	4023.

14

Deuteron-nucleus absorption cross section, mb, for -

Energy, MeV/amu	He	C	O	Al	Ar	Fe	Cu	Br	Ag	Ba	Pb
25.	438.	779.	925.	1083.	1415.	1609.	1672.	1712.	2077.	2452.	2958.
50.	319.	610.	733.	888.	1164.	1349.	1416.	1481.	1805.	2137.	2629.
75.	268.	535.	649.	801.	1055.	1235.	1303.	1377.	1684.	1997.	2481.
100.	230.	478.	583.	735.	971.	1147.	1215.	1296.	1590.	1889.	2365.
125.	209.	445.	546.	696.	923.	1096.	1164.	1248.	1534.	1825.	2297.
150.	196.	426.	523.	673.	894.	1066.	1133.	1219.	1500.	1786.	2255.
175.	187.	410.	505.	654.	870.	1041.	1109.	1196.	1474.	1756.	2222.
200.	180.	398.	491.	640.	852.	1022.	1090.	1178.	1453.	1732.	2197.
225.	174.	389.	481.	629.	839.	1008.	1075.	1164.	1437.	1714.	2177.
250.	171.	382.	473.	621.	829.	997.	1064.	1154.	1425.	1700.	2163.
275.	168.	378.	468.	616.	823.	991.	1058.	1148.	1418.	1692.	2154.
300.	167.	376.	466.	613.	819.	987.	1054.	1145.	1414.	1688.	2149.
350.	165.	373.	462.	609.	814.	981.	1049.	1139.	1408.	1681.	2141.
400.	170.	382.	472.	620.	827.	996.	1063.	1153.	1424.	1699.	2161.
500.	185.	407.	501.	650.	865.	1036.	1103.	1191.	1468.	1749.	2216.
600.	198.	429.	527.	677.	898.	1071.	1139.	1225.	1507.	1794.	2264.
700.	208.	444.	544.	695.	921.	1095.	1163.	1248.	1534.	1824.	2296.
800.	212.	451.	552.	704.	931.	1106.	1174.	1258.	1546.	1837.	2311.
900.	215.	455.	557.	709.	938.	1113.	1181.	1265.	1553.	1846.	2320.
1000.	217.	458.	560.	712.	942.	1117.	1185.	1270.	1558.	1852.	2327.
1250.	220.	463.	566.	719.	949.	1125.	1194.	1278.	1568.	1862.	2338.
1500.	221.	465.	568.	721.	952.	1128.	1197.	1281.	1571.	1866.	2342.
1750.	221.	465.	568.	721.	952.	1128.	1197.	1281.	1571.	1866.	2343.
2000.	221.	464.	567.	720.	951.	1127.	1196.	1281.	1571.	1865.	2342.
2500.	220.	463.	565.	719.	949.	1125.	1194.	1280.	1569.	1863.	2340.
3000.	219.	461.	563.	717.	946.	1123.	1191.	1277.	1566.	1860.	2336.
3500.	218.	459.	561.	715.	943.	1120.	1188.	1275.	1563.	1856.	2332.
4000.	216.	457.	558.	712.	940.	1116.	1185.	1272.	1560.	1852.	2328.
5000.	214.	454.	555.	709.	936.	1112.	1181.	1267.	1554.	1846.	2322.
6000.	213.	453.	553.	707.	934.	1109.	1178.	1265.	1552.	1843.	2319.
7000.	213.	452.	552.	706.	932.	1108.	1177.	1264.	1550.	1841.	2317.
8000.	212.	451.	551.	705.	931.	1107.	1176.	1263.	1549.	1840.	2315.
9000.	212.	450.	551.	704.	930.	1106.	1175.	1262.	1549.	1839.	2315.
10000.	212.	450.	550.	704.	930.	1105.	1174.	1262.	1548.	1838.	2314.
12500.	211.	449.	549.	703.	928.	1104.	1173.	1261.	1547.	1836.	2312.
15000.	210.	448.	547.	702.	927.	1102.	1172.	1260.	1545.	1835.	2311.
17500.	210.	447.	546.	701.	925.	1101.	1170.	1259.	1544.	1833.	2309.
20000.	209.	446.	545.	700.	924.	1100.	1169.	1258.	1543.	1832.	2308.
22500.	209.	446.	545.	700.	924.	1100.	1169.	1258.	1543.	1832.	2308.

TABLE 6. – DEUTERON-HELIUM (d-He) AND DEUTERON-CARBON (d-C) TOTAL
AND ABSORPTION CROSS SECTIONS AT 0.87 AND 2.1 GeV/NUCLEON

Collison pair	σ_{tot}, mb		σ_{abs}, mb	
	Theory	Experiment (*)	Theory	Experiment (*)
0.87 GeV/nucleon				
d-He	271	255.5 ± 3.5	214	198 ± 10
d-C	639	617.5 ± 8.2	454	411 ± 21
2.1 GeV/nucleon				
d-He	287	267 ± 5	221	204 ± 12
d-C	675	630 ± 14	464	426 ± 22

*Reference 23.
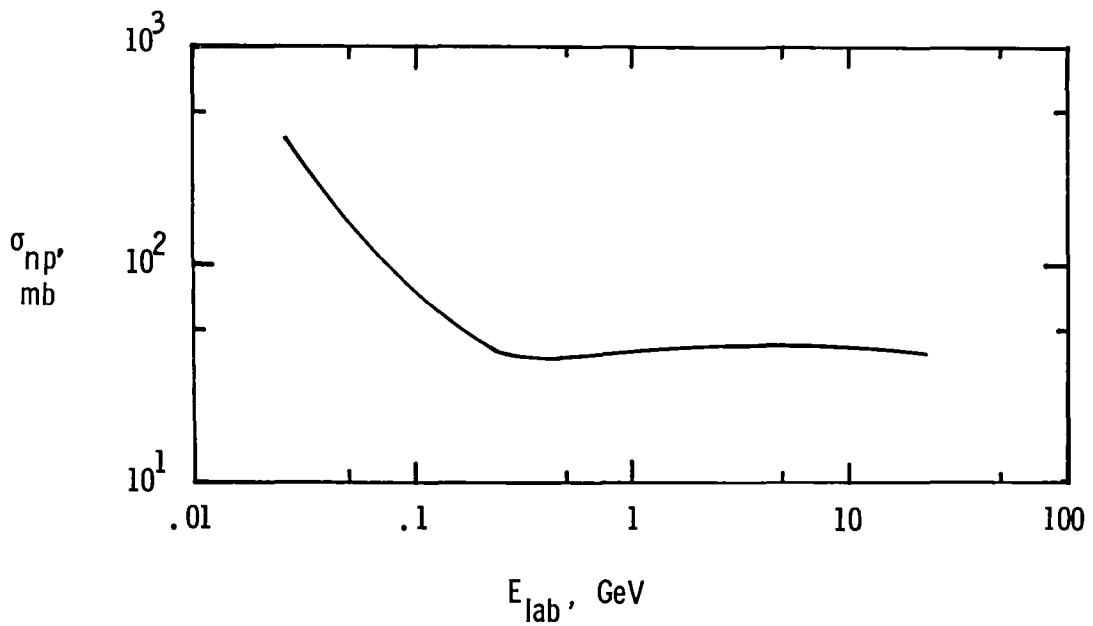
Figure 1.- Neutron-proton total cross section as a function of incident energy.
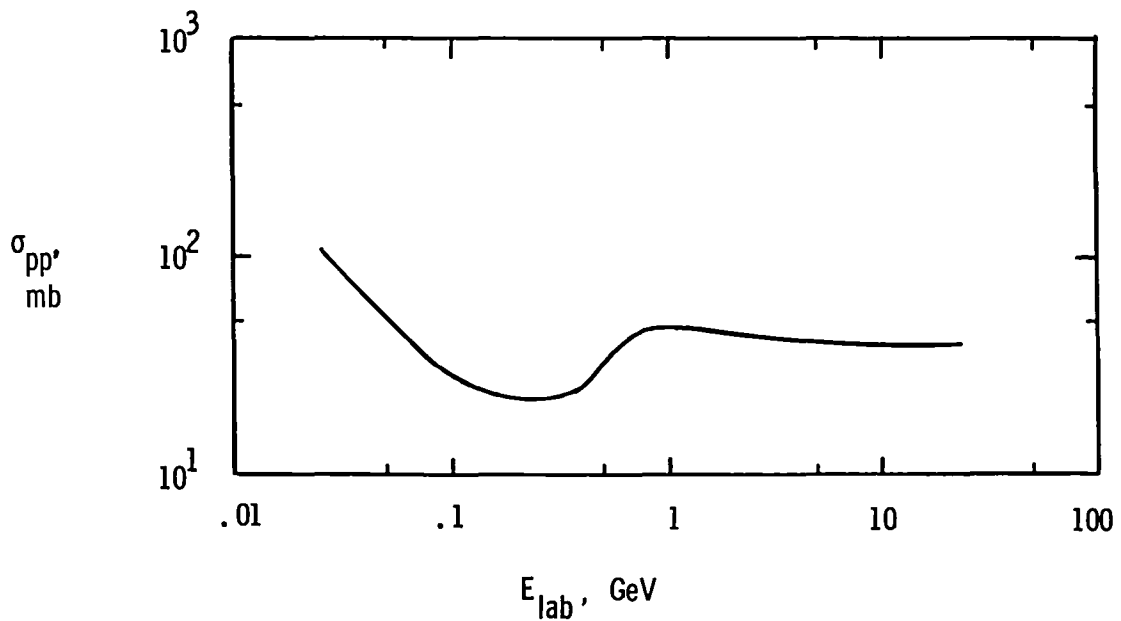
Figure 2.- Proton-proton total cross section as a function of incident energy.
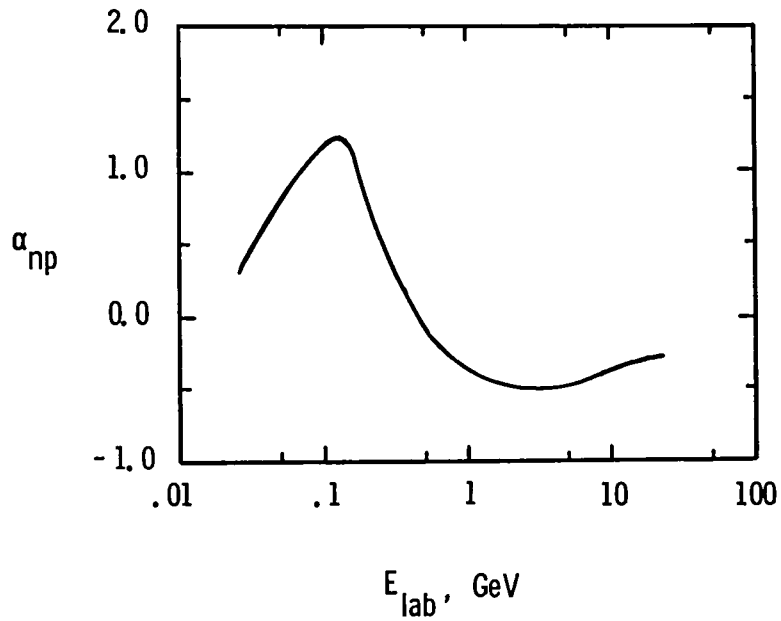
Figure 3.- Ratio of real part to imaginary part of the
forward neutron-proton scattering amplitude as a
function of incident energy.
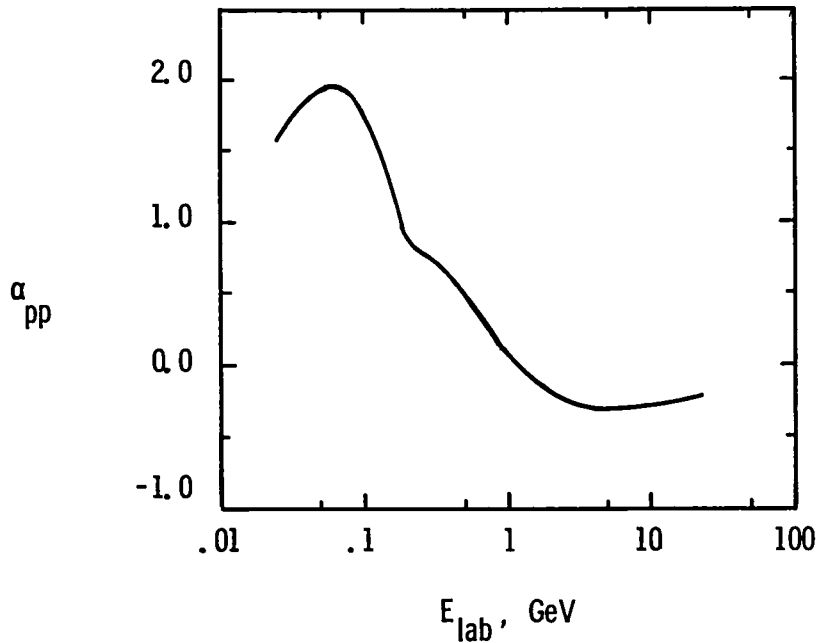
Figure 4.- Ratio of real part to imaginary part of the
forward proton-proton scattering amplitude as a
function of incident energy
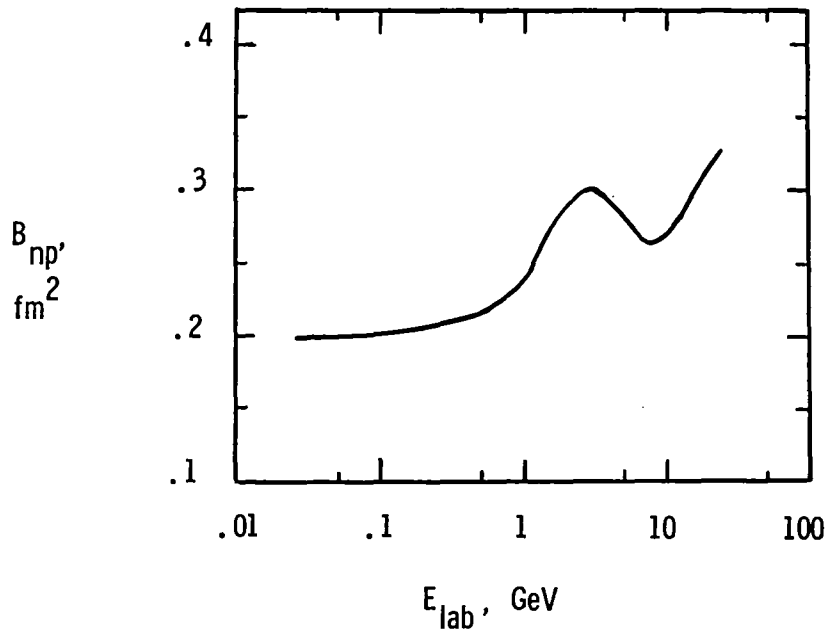
Figure 5.- Neutron-proton scattering slope parameter as a function of incident energy.
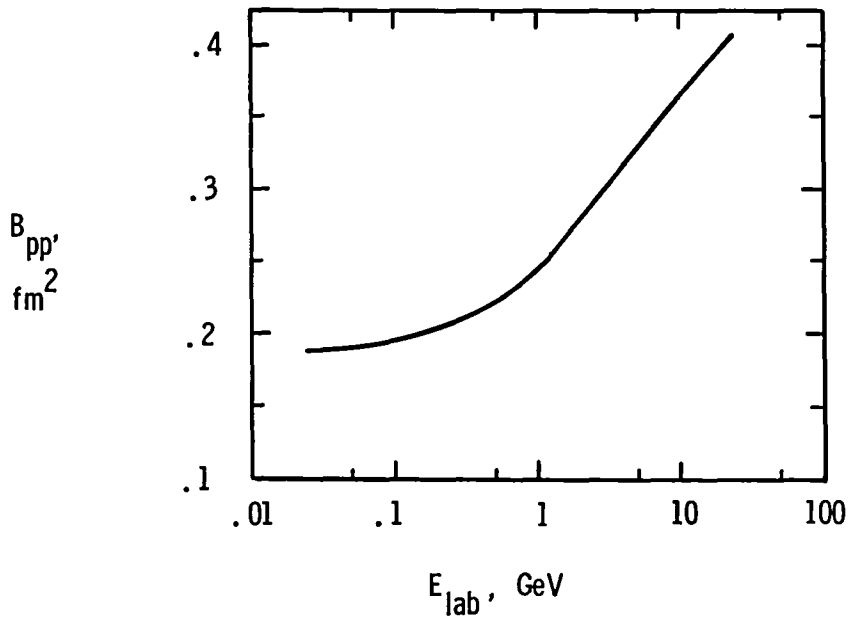
Figure 6.- Proton-proton scattering slope parameter as a function of incident energy.
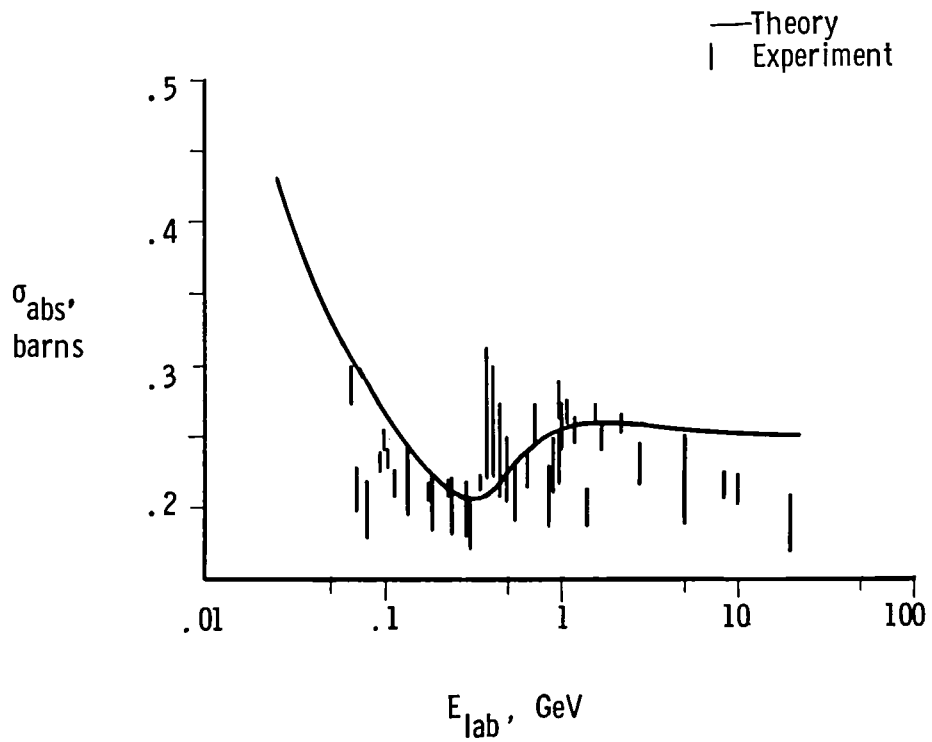
Figure 7.- Nucleon-carbon absorption cross sections as a function of incident nucleon kinetic energy.
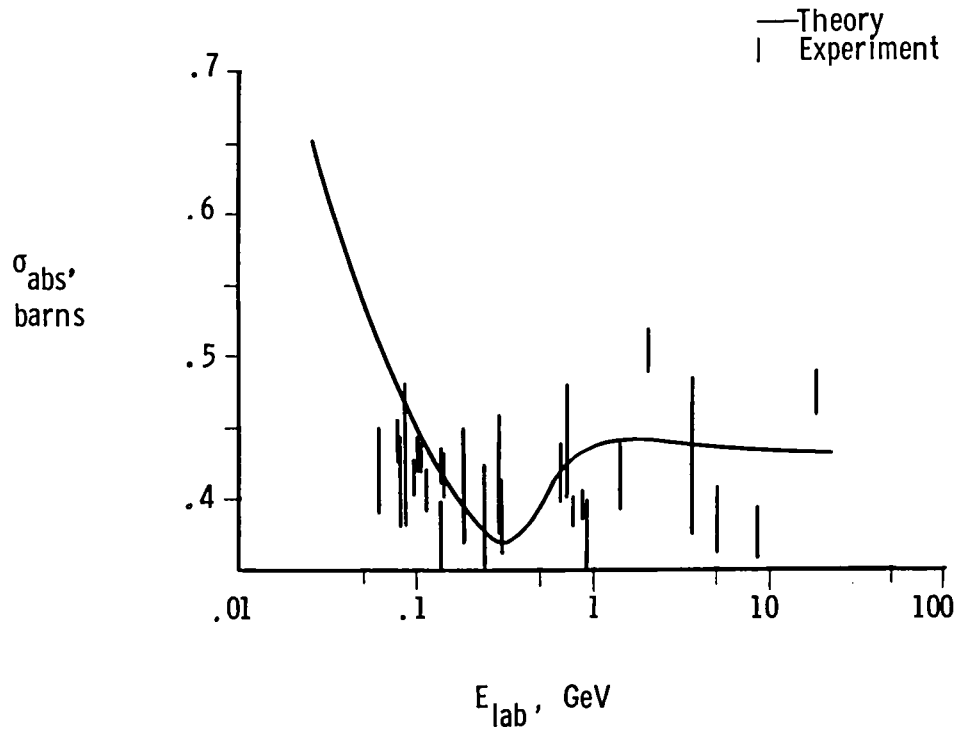
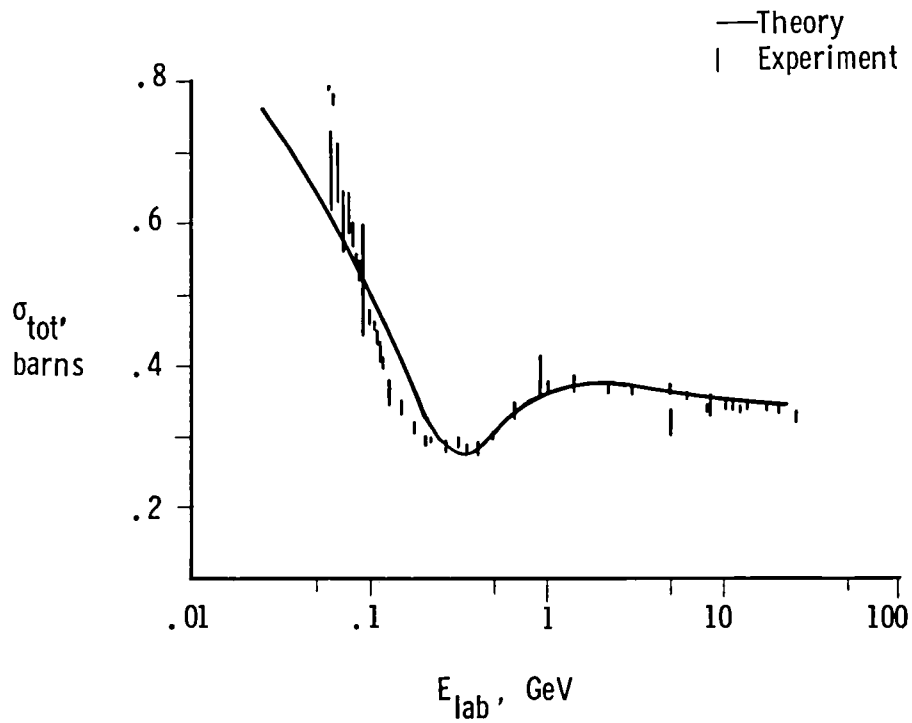Figure 8.- Nucleon-aluminum absorption cross sections as a function of incident nucleon kinetic energy.
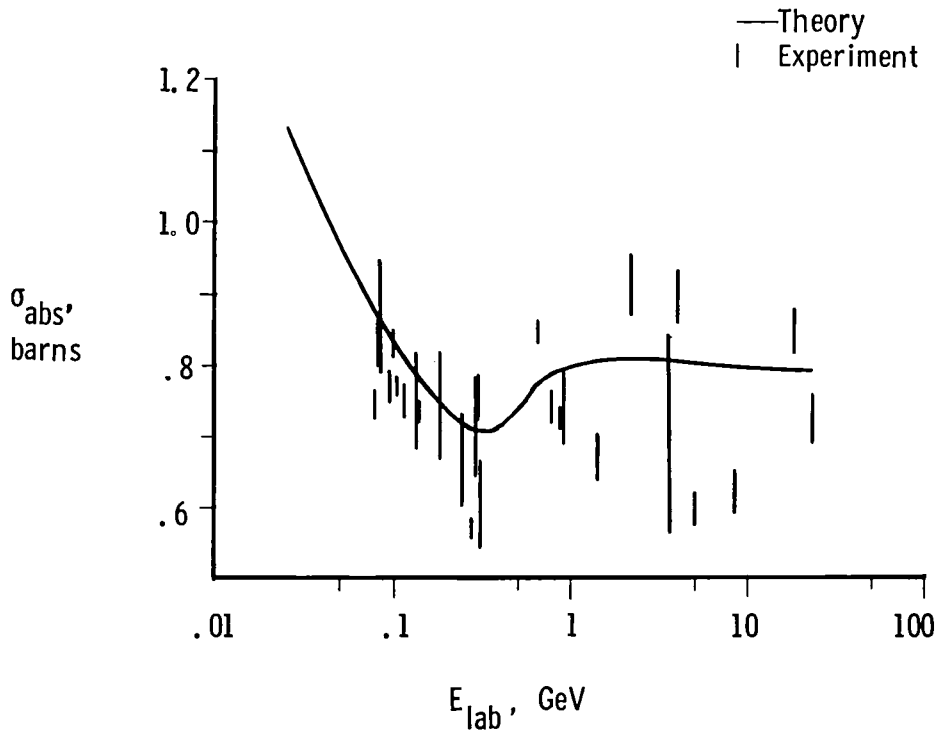
Figure 9.- Nucleon-copper absorption cross sections as a
function of incident nucleon kinetic energy.
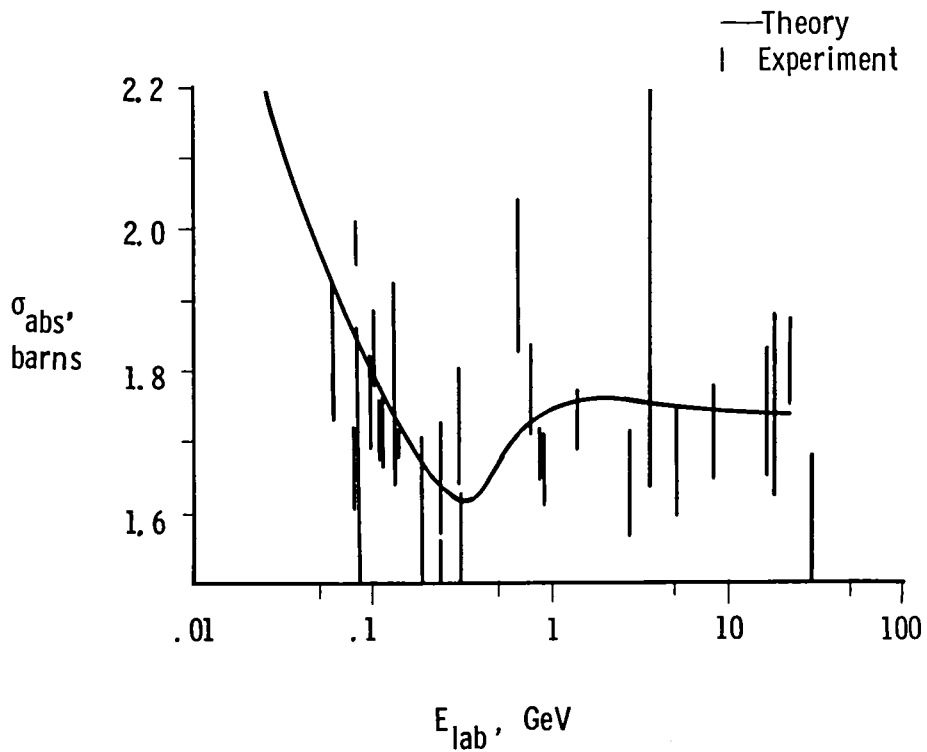
Figure 10.- Nucleon-lead absorption cross sections as a
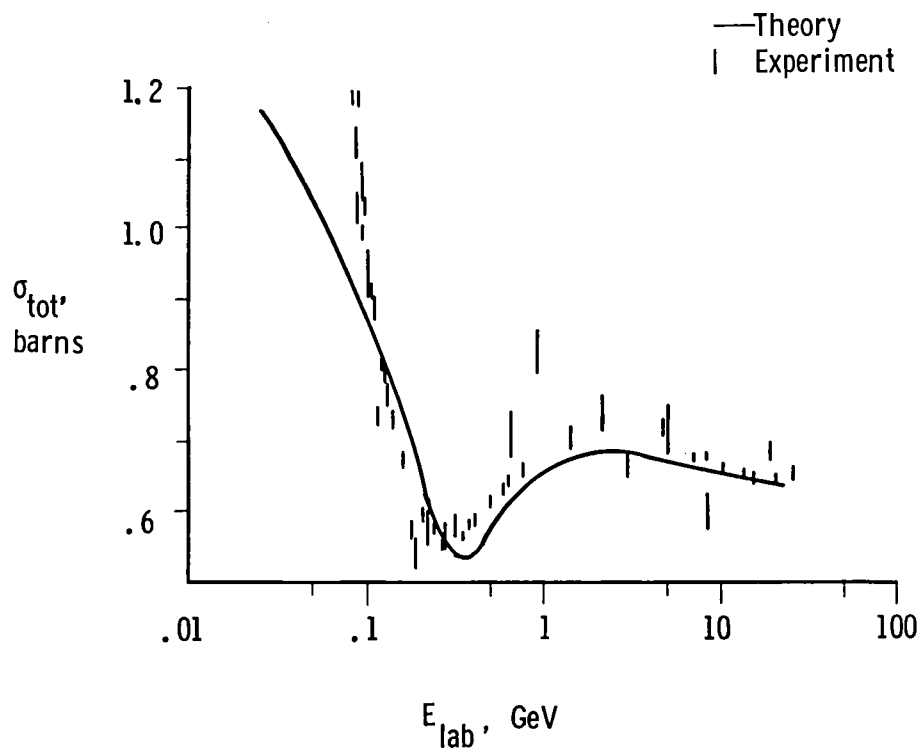function of incident nucleon kinetic energy.

Figure 11.- Nucleon-carbon total cross sections as a
function of incident nucleon kinetic energy.

Figure 12.- Nucleon-aluminum total cross sections as a
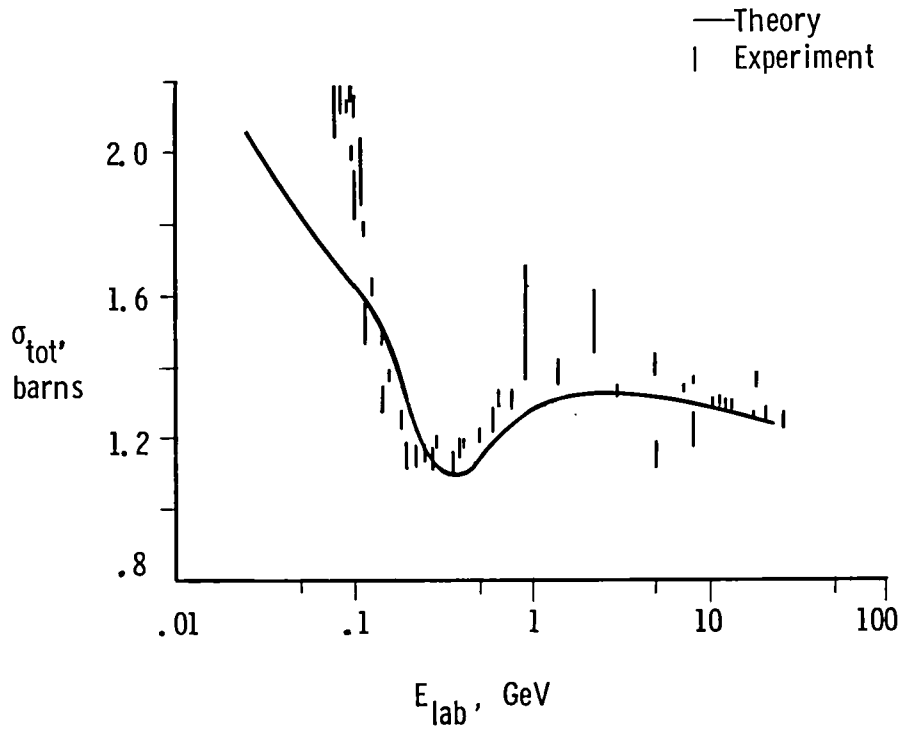function of incident nucleon kinetic energy.

22

Figure 13.- Nucleon-copper total cross sections as a function of incident nucleon kinetic energy.
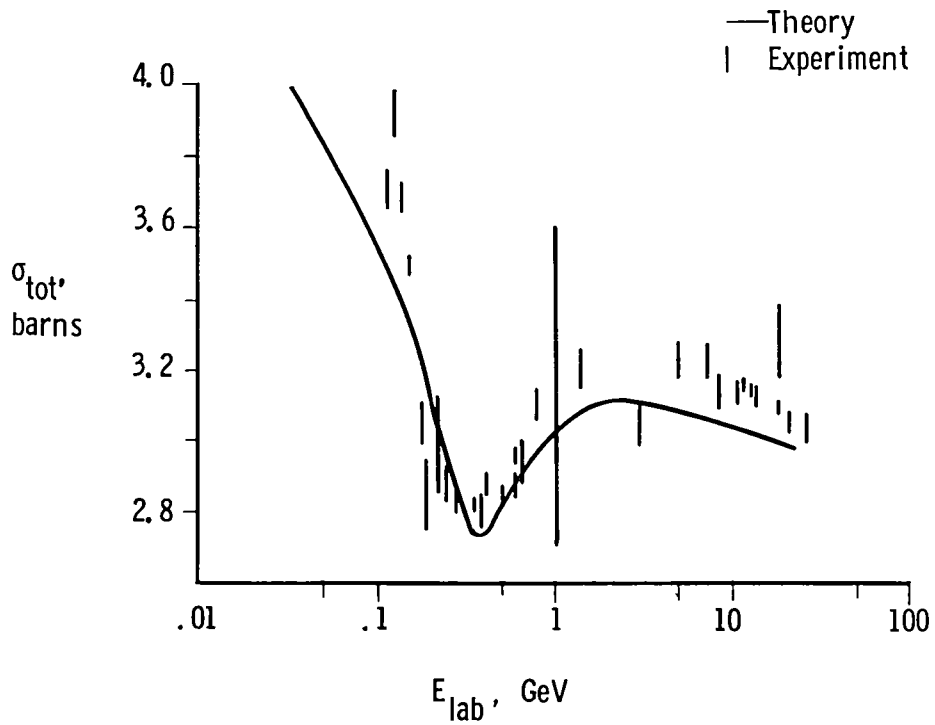

Figure 14.- Nucleon-lead total cross sections as a function of incident nucleon kinetic energy.

1. Report No. NASA TM-84636	2. Government Accession No.	3. Recipient's Catalog No.
4. Title and Subtitle NUCLEON AND DEUTERON SCATTERING CROSS SECTIONS FROM 25 MeV/NUCLEON TO 22.5 GeV/NUCLEON		5. Report Date May 1983
		6. Performing Organization Code 199-20-76-01
7. Author(s) Lawrence W. Townsend, John W. Wilson, and Hari B. Bidasaria		8. Performing Organization Report No. L-15596
		10. Work Unit No.
9. Performing Organization Name and Address NASA Langley Research Center Hampton, VA 23665		11. Contract or Grant No.
		13. Type of Report and Period Covered Technical Memorandum
12. Sponsoring Agency Name and Address National Aeronautics and Space Administration Washington, DC 20546		14. Sponsoring Agency Code

15. Supplementary Notes

Lawrence W. Townsend and John W. Wilson: Langley Research Center, Hampton, Virginia.
Hari B. Bidasaria: Old Dominion University, Norfolk, Virginia.

16. Abstract

Within the context of a double-folding optical potential approximation to the exact nucleus-nucleus multiple-scattering series, eikonal scattering theory is used to generate tables of nucleon and deuteron total and absorption cross sections at kinetic energies between 25 MeV/nucleon and 22.5 GeV/nucleon for use in cosmic-ray transport and shielding studies. Comparisons of predictions for nucleon-nucleus and deuteron-nucleus absorption and total cross sections with experimental data are also made.

17. Key Words (Suggested by Author(s)) Nucleon-nucleus scattering Deuteron-nucleus scattering Spacecraft shielding	18. Distribution Statement Unclassified - Unlimited Subject Category 73

19. Security Classif. (of this report) Unclassified	20. Security Classif. (of this page) Unclassified	21. No. of Pages 24	22. Price A02

National Aeronautics and
Space Administration

Washington, D.C.
20546

THIRD-CLASS BULK RATE

U.S.MAIL

NASA

POSTMASTER: If Undeliverable (Section 158
                Postal Manual) Do Not Return